

Evidence of Deeply Supercooled Liquid Water in Interaction with LiCl

Ryutaro Souda*

Nanoscale Materials Center, National Institute for Materials Science,
1-1 Namiki, Tsukuba, Ibaraki 305-0044, Japan

Received: March 23, 2006; In Final Form: May 8, 2006

The properties of water above the glass transition temperature are highly controversial. By using time-of-flight secondary ion mass spectrometry (TOF-SIMS), the presence of deeply supercooled water is manifested by dissolution of LiCl in the pure amorphous water films heated at 140–155 K and the formation of aqueous LiCl solutions. Two phases of deeply supercooled water, that lead to the dilute and concentrated LiCl solutions, are clearly identified. The former is short-lived and merges into the latter, whereas the latter is basically identical to normal liquid water as far as the solubility of LiCl is concerned.

Introduction

Water has been the topic of considerable research, but it still remains a mysterious material. Its peculiar physical properties may be explained by the liquid–liquid phase transition hypothesis that predicts the presence of two distinct liquid phases in the deeply supercooled region.¹ The deeply supercooled liquid water might be prepared by heating the hyperquenched glassy water (HGW) or amorphous solid water (ASW) above the glass transition temperature ($T_g = 136$ K). However, there exist significant debates not only on the assignment of T_g ^{2–6} but also on whether the glassy water converts directly to the crystal^{3–8} or first melts into the supercooled liquid.^{9,10} The traditionally assigned glass transition temperature is doubted because of the unusually small endotherm in heat capacity, and the T_g value of water has been reassigned to 165 ± 5 K from comparison of the T_g -scaled heat capacity between water and other inorganic glasses.^{3–5} In regard to crystallization, it is broadly accepted that amorphous water transforms immediately into crystalline ice Ic above 150 K,^{3–8,10–16} though the crystallographic data⁹ showed that at most 30% of water molecules crystallize in the temperature range 140–210 K. Since the crystallization should be preceded by the glass transition, the reassigned T_g value is not compatible with the crystallization at 150 K. In this respect, it was recently revealed that the ASW film dewets the Ni(111) substrate abruptly at around 160–165 K.¹⁷ The morphological change of the ASW film is caused by the long-range translational diffusion of molecules, which is characteristic of the liquid water. In reality, however, the long-range molecular diffusion is expected to occur during crystallization as well. Thus, questions still remain unresolved regarding the kinetics of glass–liquid transition and crystallization of water. These confusions would be settled if more conclusive evidence for the deeply supercooled liquid water is presented.

The liquid water can be identified by the dynamical behaviors of molecules, such as hydration of solute species. In fact, one of the most characteristic features of normal liquid water at room temperature is the formation of concentrated electrolyte solutions by dissolution of a large amount of ionic crystals. On the other hand, no electrolytes dissolve in the glassy and crystalline water due to quenching of the molecular diffusion. Therefore, more

insights into the properties of amorphous water in the deeply supercooled region would be gained from the interaction of water with electrolytes. In the present paper, we study possible dissolution of LiCl in the bulk of the pure ASW film by warming above T_g . LiCl is highly soluble in water at room temperature, and the concentrated solution can be vitrified without phase separation,^{18,19} thereby enabling us to discuss the properties of the LiCl solutions over a wide temperature range. If the aqueous LiCl solution is formed in the deeply supercooled regime at the well-defined interface between the pure water and LiCl films, it can be ascribed undoubtedly to the presence of supercooled liquid water. We analyze the compositional change of the pure ASW films deposited on the LiCl film by using time-of-flight secondary ion mass spectrometry (TOF-SIMS) in the temperature range 140–155 K and discuss whether the supercooled liquid water, if any, is a thermodynamic extension of normal water or a distinct phase.

Experimental Methods

The experiments were performed in an ultrahigh-vacuum (UHV) chamber of base pressure below 1×10^{-9} Pa. A pulsed He⁺ beam (2.0 keV, ~ 10 pA/cm²) was incident on the sample which was floated with a bias voltage of 500 V, and the secondary ions extracted into a field-free flight tube were accumulated every 30 s to make a TOF-SIMS spectrum under the isothermal and temperature-programmed modes. The Ni(111) surface has been used as a substrate because dewetting of the ASW film during the glass–liquid transition can be identified in the TOF-SIMS experiments from the emission of the Ni⁺ and Ni⁺(H₂O)_n ions.¹⁷ The Ni(111) sample was spot-welded to the Ta holder using a Ni sheet. The sample was inserted in the UHV chamber via a load-lock system. Cooling of the sample was achieved by thermal contact between the mirror-finished faces of the Ta holder and a sapphire plate that was attached to the copper block cooled to 13 K by means of a closed-cycle helium refrigerator. Heating was achieved by electron bombardment from behind through a square hole opened in the sapphire plate. The Ni(111) surface was cleaned by heating at 1200 K, and LiCl was deposited on it with a thickness of approximately 500 nm at room temperature. The nonporous ASW film was grown on the Ni(111) and LiCl surfaces at 100 K by backfilling the UHV chamber with the

* E-mail: SOUDA.Ryutaro@nims.go.jp.

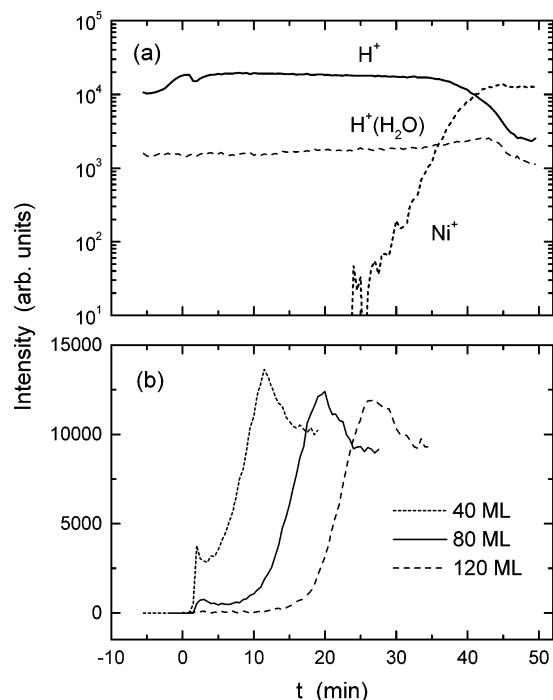


Figure 1. (a) Isothermal TOF-SIMS intensities of typical secondary ions from the water-deposited Ni(111) surface at 155 K. The H_2O molecules with a thickness of 200 ML (~ 35 nm) were deposited on the clean Ni(111) surface at 100 K. After deposition of water, the sample was heated to 155 K at a rate of 8 K/min. The negative time corresponds to the sample heating stage. (b) Isothermal TOF-SIMS intensities of the Ni^+ ion at 155 K when the thinner ASW films (40, 80, and 120 ML) are deposited on the Ni(111) surface.

H_2O gas. One-monolayer (1 ML) coverage of the H_2O molecules was determined from the evolutions of the sputtered H^+ , $H^+(H_2O)$, and Ni^+ intensities as a function of exposure, and the film thickness was determined on the basis of this value. The sample was heated at a rate of 8 K/min to temperatures for the isothermal TOF-SIMS measurements. The spectra were taken continuously at fixed temperatures with an accuracy of ± 1 K.

Results

Figure 1a shows isothermal TOF-SIMS intensities of H^+ , $H^+(H_2O)$, and Ni^+ ions from the Ni(111) surface on which the ASW film with a thickness of 200 ML (~ 35 nm) was deposited. The negative time corresponds to the sample heating stage from 100 to 155 K. The H^+ intensity increases during heating, and then, a dip occurs within 2 min after 155 K is reached. In contrast, the $H^+(H_2O)$ intensity is almost constant in this temperature range. This phenomenon has been explained in terms of the glass–liquid transition of the ASW film.²⁰ The H^+ ions are emitted mainly from lone hydrogen atoms of H_2O without hydrogen bonds due to breakage of the partly ionic $-OH$ bond, while the $H^+(H_2O)$ ion stems from the collision-induced hydrolysis of water molecules, $2H_2O \rightarrow H^+(H_2O) + OH^-$. Therefore, the structure of the film changes at the molecular level during the glass–liquid transition (structural relaxation) due to the reorganization of hydrogen bonds between the water molecules. At this break point, the morphology of the fluidized film changes due to the surface tension, as evidenced by the occurrence of dewetting of the films.²⁰ The dewetting is observed clearly for the thinner water films: Figure 1b shows the time evolutions of the Ni^+ intensities in the isothermal TOF-SIMS experiment for the water (<120 ML)-

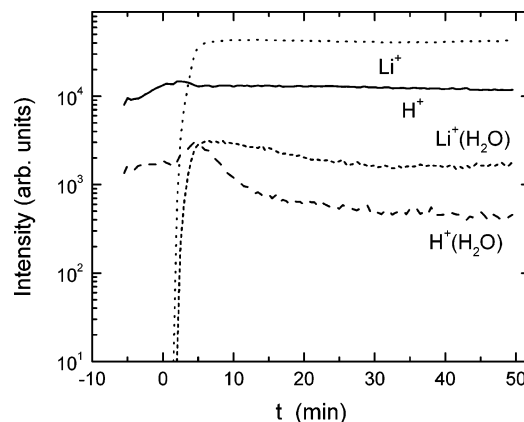


Figure 2. Isothermal TOF-SIMS intensities from the water (200 ML)-deposited LiCl film (~ 500 nm) at 155 K. The measurements were made under the same conditions as those in Figure 1a.

adsorbed Ni(111) surface at 155 K. The Ni^+ ion is emitted from the Ni(111) substrate concomitantly with the occurrence of the dip in the H^+ intensity. The dewetting is caused by reconstruction of the water molecules with a thickness of ~ 100 ML, so that the Ni(111) surface is not exposed when it is covered with the thicker ASW films.

The morphological change of the ASW film should be induced by the long-range translational diffusion of the water molecules. This behavior is expected for the fluidized film, but the molecular diffusion is prerequisite for crystallization as well. The crystallization of water has been discussed extensively in the studies of temperature-programmed and isothermal desorption,^{10–14} in which the desorption rate of water molecules from the crystalline phase is presumed to be much lower than that from the amorphous phase. The desorption rate of water molecules decreases abruptly at around 145–150 K (isothermal experiment) and 160 K (temperature-programmed experiment), and this behavior has been explained in terms of the crystallization of the ASW film. On the other hand, it is claimed that the morphological change of the ASW film induces the drop in the desorption rate of water molecules.^{17,20}

To assign this phenomenon precisely, the interaction of the ASW film with LiCl has been studied. Figure 2 shows the isothermal TOF-SIMS intensities (155 K) from the 200 ML ASW film deposited on the LiCl film at 100 K; the measurement was made under the same conditions as those in Figure 1a. It should be noticed that the intensity of the Li^+ ion increases steeply, together with its hydrated ions, $Li^+(H_2O)$, after the morphological change of the film occurs at 1.5–2 min. The $H^+(H_2O)$ ion decreases considerably after the evolution of Li^+ . This behavior is caused by intermixing of water with LiCl and cannot be ascribed to dewetting of the water film. In fact, the $Li^+(LiCl)$ ion, which is emitted from the clean LiCl film, is not observed at all in this experiment. Therefore, these results indicate that pure supercooled liquid water forms first and then LiCl dissolves in it. The resulting aqueous LiCl solution survives in a vacuum for a longer time than the pure water (see Figure 1a). This is because the activity of water molecules in the solution (hence the vapor pressure) is very much lowered than that in pure water due to a large decrease in free energy.

Figure 3a shows results of the temperature-programmed TOF-SIMS experiment performed successively after the isothermal TOF-SIMS measurement (Figure 2). The $H^+(H_2O)$ ion decreases in intensity by heating, and the $Li^+(LiCl)$ ion evolves at 186 K, where the unhydrated patches of LiCl begin to appear due

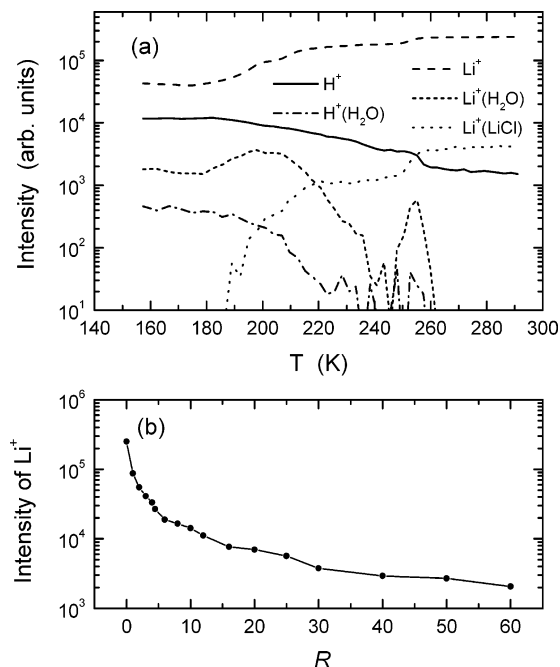


Figure 3. (a) Temperature-programmed TOF-SIMS intensities of typical secondary ions sputtered from the water-adsorbed LiCl thin film, which was taken successively after the measurement of Figure 2. The temperature was ramped at a rate of 5 K/min. (b) The calculated Li^+ intensities as a function of the R value of nominal solutions of $\text{LiCl} \cdot R\text{H}_2\text{O}$. The surface sputtering simulations were performed by using the SRIM code.²¹ The density of aqueous LiCl solution was assumed as a mean value of water (1.0 g/cm^3) and LiCl (2.07 g/cm^3).

to evaporation of the H_2O molecules from the aqueous LiCl solution or exposure of the LiCl film. The $\text{Li}^+(\text{LiCl})$ ion should not be created from the LiCl solution because the Li^+ and Cl^- ions are hydrated by the water molecules. The multilayer of pure water formed on the Ni(111) substrate evaporates completely at 180–185 K, as revealed by a drop in the $\text{H}^+(\text{H}_2\text{O})$ intensity (not shown explicitly), whereas the $\text{H}^+(\text{H}_2\text{O})$ and $\text{Li}^+(\text{H}_2\text{O})$ ions in Figure 3a remain considerably above 185 K due to survival of some hydrates on the LiCl surface. The Li^+ and $\text{Li}^+(\text{LiCl})$ ions increase in intensity stepwise via at least four stages due to dehydration. The dehydration is completed at around 250–260 K, which corresponds to the peritectic point (252.6 K), as observed by warming the quenched LiCl solution.^{18,19}

In general, the secondary ion yield is controlled so sensitively by the matrix effect due to the ionization and neutralization of ions at the surface that the quantitative compositional analysis by SIMS is usually difficult. In the present case, however, Li^+ ions in the highly insulating materials are sputtered without suffering from neutralization because of the presence of a large band gap. The composition of aqueous solutions, $\text{LiCl} \cdot R\text{H}_2\text{O}$, where R is the number of water molecules per mole of LiCl, can be determined by the Li^+ yield from the solutions relative to that from the pure ionic LiCl crystal after complete dehydration. The sputtering yield of Li^+ was calculated using the SRIM code.²¹ The normalized Li^+ intensities are plotted in Figure 3b as a function of R . The experimental Li^+ intensity from the supercooled aqueous LiCl solution is reproduced by the nominal composition of $\text{LiCl} \cdot 3\text{H}_2\text{O}$. This solution should be glassy at 155 K, since T_g increases from 136 to 165 K when the LiCl concentration increases from $R = 5$ to $R = 3$.^{18,19}

In Figure 4 is shown the H_2O thickness dependence of the evolution of the Li^+ intensity observed at 155 K. The morphology of the film changes at 1.5–2 min irrespective of the

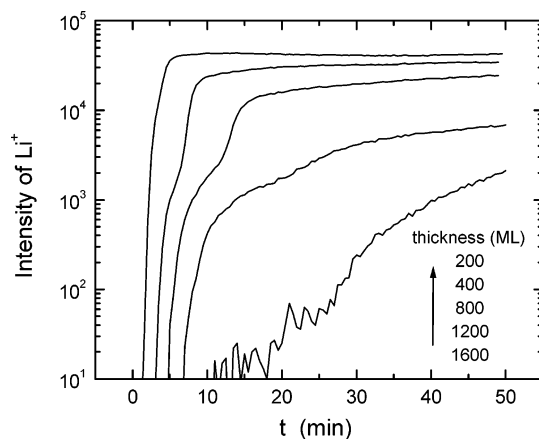


Figure 4. Time evolutions of the Li^+ intensities from the water-adsorbed LiCl films. The measurements were made at 155 K for the water films with different thicknesses.

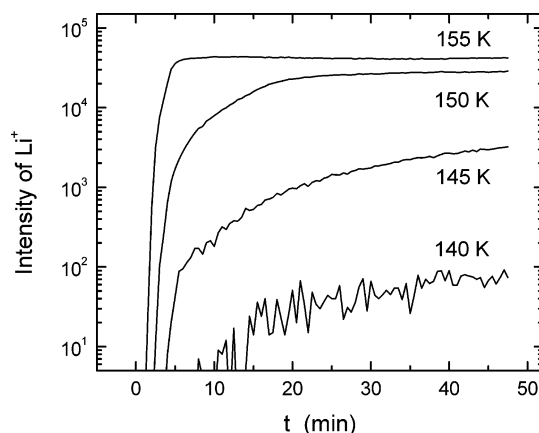


Figure 5. Time evolutions of the Li^+ intensities from the water (200 ML)-deposited LiCl films at several temperatures above $T_g = 136 \text{ K}$.

thickness, as determined from the dip in the H^+ intensity. In addition to the 200 ML water film, the Li^+ intensity seems to be saturated for the 400 ML film ($R = 4$, $T_g = 152 \text{ K}$) as well due to freezing into the glassy state after formation of the aqueous LiCl solution. The concentration of LiCl increases toward the interface, so that such glassy layers should be buried underneath the thicker films, thereby slowing down the Li^+ evolution speed with increasing thickness of the initial ASW film. An interesting feature is seen for the intermediate thickness films (400–1200 ML), in which a very dilute solution ($R > 50$) emerges first and then a concentrated one follows. This result suggests that two liquid phases characterized by different solubilities of LiCl exist in the deeply supercooled regime.

Figure 5 shows the time evolution of the Li^+ intensity from the water (200 ML)-deposited LiCl film measured at several temperatures above the conventional T_g value (136 K). The LiCl solution is formed within minutes, as revealed from the evolution curves of the Li^+ ion, though the diffusivity of LiCl is lowered considerably when approaching T_g . Similar to the result at 155 K, the final product at 150 K has such a high LiCl concentration ($R = 4$ –5, $T_g = 145$ –150 K) that it may freeze into the glassy state. From these experimental results, we can assign T_g undoubtedly to 135–140 K, though a considerably long aging time ($\sim 10 \text{ min}$) is necessary for the occurrence of structural relaxation.²⁰ The LiCl concentration increases gradually at 145 K without freezing, indicating that the supercooled liquid phase has a considerably long lifetime (see also Figure 4).

Discussion

The presence of the supercooled liquid water is manifested by the dissolution of LiCl in the deeply supercooled regime. The resulting LiCl solutions may be linked to the LiCl solutions at room temperature. It is known that the concentrated LiCl solutions can be supercooled without phase separation but dilute LiCl solutions ($R > 12$) are hardly obtained.^{18,19} This is because the dilute solutions are unstable at low temperatures and split into two phases, that is, concentrated solution and pure amorphous water (HW).^{22,23} The dilute LiCl solution ($R > 50$) observed here is formed provided that deeply supercooled liquid water interacts with LiCl at the very beginning of the glass–liquid transition. This liquid phase is short-lived and merges into the second liquid phase that is characterized by a much higher solubility of LiCl. The presence of two supercooled liquid phases invokes the hypothesis of a second critical point:^{1,24,25} pure liquid water separates into hypothesized low- and high-density liquid (LDL and HDL) phases in its deeply supercooled region, and they become the known low- and high-density amorphous ices (LDA and HDA) at lower temperatures.²⁶ It is considered that this hypothesis is hardly evidenced experimentally by using bulk water because of the crystallization of the liquid water. Here, we demonstrate that the supercooled liquid water (LDL) is accessible from the low-temperature side by heating the ASW (which is identical to LDA after annealing) above T_g . Although little is known about the properties of LDL, the local structure of LDA is quite similar to (largely different from) that of crystalline ice Ih (liquid water).²⁷ This fact suggests that LDL is characterized by a poor solubility of electrolytes. The LDL is thought to be identified as the “ultraviscous water” that exists from the onset of molecular diffusion ($T_g = 136$ K) until the occurrence of the second liquid phase that induces the morphological change of the film. Indeed, there exist no structural discontinuities of water at T_g (LDA \rightarrow LDL) except for the enhanced diffusivity of water molecules. In this respect, moreover, it was revealed that the alkenes, which are accommodated in the bulk of the ASW film at lower temperatures, survive in the ultraviscous liquid phase above T_g .²⁸ This occurs because LDL can be regarded as a tetrahedrally structured liquid that can dissolve hydrophobic molecules.²⁹ The incorporated alkanes are released concomitantly with the morphological change of the film,²⁸ whereas the second phase of supercooled liquid water, characterized by the long-range diffusivity of molecules, can dissolve a large amount of LiCl. According to the second critical point hypothesis,¹ the properties between the LDL and HDL are distinguishable below the critical point, $T_c = 220$ K and $P_c = 100$ MPa, so that the liquid water at 155 K should be assigned to LDL. In this respect, the birth of the second liquid phase in the deeply supercooled region is noticeable. Its properties, that is, the high solubility of LiCl ($R = 3$ –4) and the poor solubility of alkanes, are characteristic of normal liquid water. Thus, it is concluded that the LDL is short-lived, since it develops into supercooled normal liquid or freezes into crystalline ice Ic.

The present result also conflicts with the conventional belief that the ASW or LDA freezes immediately into crystalline ice Ic above 145–150 K.^{3–16} They are based on the calorimetric^{3–5} and dielectric⁶ studies, FT-IR,⁷ and the proton-transfer measurement.⁸ The same conclusion is reached by the thermal desorption studies,^{10–16} but it is due to the misleading assignment of the morphological change of the film to crystallization, as already mentioned. The isotope scrambling⁷ and the related proton transfer⁸ above 140–150 K should be caused by the self-diffusion of water molecules in the supercooled liquid phase.

On the other hand, the conclusion of the calorimetric studies^{3–5} that the glass transition endotherm is absent up to 150 K may be true. In the temperature-programmed TOF-SIMS experiments,^{17,28} the film morphology changes at around 160–165 K because the conversion of ultraviscous water (LDL) to the second liquid phase (normal liquid water) requires some aging time depending on the temperature (see also Figure 5). As a consequence, it is likely that the glass transition endotherm is overlapped with the huge crystallization exotherm ($T > 150$ K), thereby masking the real glass transition of water in the calorimetric study. Thus, the controversies on water's T_g value can be attributed to the kinetic problems in the crystallization and glass–liquid transition.²⁰

Here, we do not present the direct experimental evidence for the glass transition of pure water, but the evolution of deeply supercooled liquid water should be responsible for the dissolution of LiCl. The supercooled liquid phases are unstable for both pure water and LiCl solution because of ice nucleation. However, there exist wide metastable regions for the supercooled LiCl solutions due to the slow ice crystallization in the time scale of hours or days.^{18,19} Although the lifetime of the pure supercooled water may be shorter than the supercooled LiCl solutions, the highly concentrated solutions are not expected to form unless the supercooled liquid is dominant over the crystal ice Ic above T_g .

Conclusion

The formation of the deeply supercooled liquid water has been discussed on the basis of the interactions between the thin films of ASW and LiCl. The morphology of the ASW film changes above $T_g = 136$ K after some aging time depending on the temperature. This behavior is interpreted by the occurrence of the long-range translational diffusion of water molecules due to the evolution of deeply supercooled liquid water. This is evidenced by the fact that LiCl dissolves in the fluidized water film after structural relaxation. It is found that the dilute LiCl solution evolves first and then the concentrated one follows. The former is hardly accessible by quenching the aqueous LiCl solutions formed at room temperature due to the phase separation, whereas the latter is basically identical to the quenched LiCl solutions. This result suggests that two distinct liquid phases exist in the deeply supercooled regime; the first liquid phase, characterized by a poor solubility of LiCl and a high solubility of hydrophobes, is thought to be LDL, and the second liquid phase may be linked directly to the normal liquid water, as inferred from the high solubility of LiCl. The glass–liquid transition at 136 K is followed by the liquid–liquid transition in the deeply supercooled region. It is thus demonstrated that the supercooled aqueous solutions can be prepared by heating the water-deposited thin films of solute species above T_g and that the slowed-down molecular dynamics of the aqueous solution can be explored on real time under vacuum conditions.

References and Notes

- (1) Mishima, O.; Stanley, H. E. *Nature* **1998**, 396, 329.
- (2) Johari, G. P.; Hallbrucker, A.; Mayer, E. *Nature* **1987**, 330, 552.
- (3) Velikov, V.; Borick, S.; Angell, C. A. *Science* **2001**, 294, 2335.
- (4) Yue, Y.; Angell, C. A. *Nature* **2004**, 427, 717.
- (5) Giovambattista, N.; Angell, C. A.; Sciortino, F.; Stanley, H. E. *Phys. Rev. Lett.* **2004**, 93, 047801.
- (6) Minoguchi, A.; Richert, R.; Angell, C. A. *Phys. Rev. Lett.* **2004**, 93, 215703.
- (7) Fisher, M.; Devlin, J. P. *J. Phys. Chem.* **1995**, 99, 11584.
- (8) Cowin, J. P.; Tsekouras, A. A.; Iedema, M. J.; Wu, K.; Ellison, G. B. *Nature* **1999**, 398, 405.

- (9) Jenniskens, P.; Banham, S. F.; Blake, D. F.; McCoustra, M. R. *J. Chem. Phys.* **1997**, *107*, 1232.
- (10) Smith, R. S.; Kay, B. D. *Nature* **1999**, *398*, 788.
- (11) Kouchi, A. *Nature* **1987**, *330*, 550.
- (12) Smith, R. S.; Huang, C.; Wong, E. K. L.; Kay, B. D. *Surf. Sci.* **1996**, *367*, L13.
- (13) Lofgren, P.; Ahlstrom, P.; Chakarov, D. V.; Lausmaa, J.; Kasemo, B. *Surf. Sci.* **1996**, *367*, L19.
- (14) Smith, R. S.; Huang, C.; Wong, E. K. L.; Kay, B. D. *Phys. Rev. Lett.* **1997**, *79*, 909.
- (15) Safarik, D. J.; Meyer, R. J.; Mullins, C. B. *J. Chem. Phys.* **2003**, *118*, 4660.
- (16) Backus, E. H. G.; Grecea, M. L.; Kleyn, A. W.; Bonn, M. *Phys. Rev. Lett.* **2004**, *92*, 236101.
- (17) Souda, R. *Phys. Rev. Lett.* **2004**, *93*, 235502.
- (18) Elarby-Aouizerat, A.; Jal, J.-F.; Chieux, P.; Letoffe, J. M.; Claudy, P.; Dupuy, J. *J. Non-Cryst. Solids* **1988**, *104*, 203.
- (19) Prevel, B.; Jal, J. F.; Dupuy-Philon, J.; Soper, A. K. *J. Chem. Phys.* **1995**, *103*, 1886.
- (20) Souda, R. *Chem. Phys. Lett.* **2005**, *415*, 146.
- (21) Ziegler, J. F.; Biersack, J. P.; Littmark, U. In *The Stopping and Range of Ions in Solids*; Pergamon Press: New York, 1985.
- (22) Angell, C. A.; Sare, E. J. *J. Chem. Phys.* **1968**, *49*, 4713.
- (23) Suzuki, Y.; Mishima, O. *Phys. Rev. Lett.* **2000**, *85*, 1322.
- (24) Poole, P. H.; Sciortino, F.; Essmann, U.; Stanley, H. E. *Nature* **1992**, *360*, 324.
- (25) Debenedetti, P. G. *Nature* **1998**, *392*, 127.
- (26) Mishima, O.; Calvert, L. D.; Whalley, E. *Nature* **1984**, *310*, 393.
- (27) Finney, J. L.; Hallbrucker, A.; Kohl, I.; Soper, A. K.; Bowron, D. T. *Phys. Rev. Lett.* **2002**, *88*, 225503.
- (28) Souda, R. *J. Chem. Phys.* **2004**, *121*, 8676.
- (29) Paschek, D. *Phys. Rev. Lett.* **2005**, *94*, 217802.